Journal of the European Ceramic Society, Volume 26, Issues 1-2, 2006, Pages 117-123.

Preparation Of Sub-Micron PZT Particles With The Sol-Gel Technique.

S. Linardos*, Q. Zhang and J. R. Alcock

Advanced Materials Department, School of Industrial and Manufacturing Science, Cranfield University, Bedfordshire MK43 0AL, UK

Abstract

This paper describes the production of $Pb_{1.0}Zr_{0.9}Ti_{0.1}$ ceramic powder, by using metal organic precursors as starting materials. In this study polyvinylpyrrolidone, PVP, was used to create a PZT-PVP sol and then also added as a secondary stage to control the particle size of the powder.

Two different sol-gel routes were used to create PZT powder. Both routes gave similar primary particle sizes in the range, 30 - 70 nm, but different agglomerate formations. Perovskite PZT powder was created with both routes.

Keywords : A. Powders-chemical preparation, A. Sol-gel processes, D. PZT

* Corresponding author. Fax: +44 (0) 1234 752473
E-mail addresses: s.linardos.2001@cranfield.ac.uk (S. Linardos)
j.r.alcock@cranfield.ac.uk (J. R. Alcock)

Introduction

In advanced ceramics the size, size distribution, shape and state of agglomeration of the starting powder strongly affect the microstructure of the sintering body, and the temperature at which it densifies [1]

Lead Zirconate Titanate (PZT) is an important ferroelectric material, widely used for its piezoelectric and pyroelectric properties. There are a variety of methods for the preparation of PZT powder. Mechanochemical synthesis [2]-[5], chemical synthesis [6]-[10] or hydrothermal synthesis [11]-[14] has each been successfully used.

Processing routes for the production of monodispersed fine powders are becoming increasingly common. TiO_2, ZrO_2 and SiO_2 were some of the first powders to have been successfully created [15]-[19] with the sol-gel technique. The synthetic methods used to prepare these materials involve fairly simple solution chemistry, however they give a high degree of control and reproducibility.

However, it is more difficult to create monodispersed particles with two or more metallic elements because of the tendency of one of the metal alkoxides to precipitate out of the solution more quickly than the other. This is owing to differences in hydrolysis rates of the alkoxides.

A sol-gel technique has previously been used by several authors [20]-[26] to create a PZT powder.

In this paper a new sol-gel route for PZT, incorporating polyvinylpyrrolidone, PVP, is presented. PVP has previously been used with success for the creation of crack free thick, and thin films [27]-[28] and in

some cases to improve the properties of the final powders [29]-[30]. In this study PVP, was used both to create a PZT-PVP sol and also as a secondary stage to control the particle size of the powder produced.

The advantage of this new sol-gel route is the capability of producing controlled nano-scale ceramic powder with specific crystalline phase.

Experimental

The preparation route of the $Pb_{1.0}Zr_{0.9}Ti_{0.1}$-PVP gel (i) is shown in Figure 1.

To produce 160 ml of sol, the following route was used. 12.14 g of lead(II) acetate trihydrate was left under vacuum at 100 ^{o}C for 24 hours to remove the water. 12.21 g of zirconium(IV) propoxide, 76.33% by weight in n-propanol, and 0.9 g of titanium(IV) isopropoxide were dissolved in 120 ml isopropanol. This mixture was heated to 80 ^{o}C under stirring. After three hours the lead(II) acetate was added. The mixture was stirred for another three hours under the same conditions. Extra isopropanol was added until the final volume of the solution reached the 160 ml. A light-transparent PZT sol was obtained. To transform this into a PZT-PVP sol, 5.5 g of PVP with average molecular weight of 1 300 000 were added and the stirring was continued until it became clear yellow in colour.

The resulting PZT-PVP sol had a concentration of 0.2 M of lead. The $Pb(OAc)_2$: PVP weight ratio of the sol was 1 : 0.5. In order to hydrolyse this to produce a gel, water was slowly added up to the maximum of $[H_2O]/[Pb]$ = 0.66. A PZT-PVP gel, gel (i), was obtained.

Subsequent to these common processing steps, two processing routes, here called A and B were followed.

Powder preparation route A is shown in Figure 2a. The PZT-PVP gel (i) was left to dry at 60 ^{o}C for 144 h and then burnt out at 500 ^{o}C for 1h. An orange coloured powder was created.

Powder preparation route B is shown in Figure 2b. The PZT-PVP gel (i) was stirred for 10 min at 1200 rpm, and then 0.2 g of PVP with average molecular weight 55 000 was added per millilitre of sol. The new PZT-PVP gel, gel (ii), was dried at 60 ^{o}C for 144 h and then heat treated at two different profiles, one at 500 ^{o}C for 1 hour and the second at 550 ^{o}C for 24 hours.

A Philips XL series Scanning Electron Microscope and a Siemens D5005 X-Ray Diffractometer were used for sample analysis.

Size measurements of the powder were performed using a Zeta-Sizer 3000 (Malvern Instruments). Each powder before the measurements was diluted in water and left in an ultrasound bath for 40 min.

Differential scanning calorimetry of the gels was performed using a modulated DSC (TA Instruments) model 2920. A constant heating rate of 10 ^{o}C min^{-1} from 20 to 450 ^{o}C was used, with an isothermal dwell at 450 ^{o}C for 60 min. All the measurements took place under a constant nitrogen flow. Hermetic aluminium pans were used to encapsulate the samples.

Results

Figures 3a - 3b are SEM micrographs of typical PZT powder that was produced using route A. In Figure 3a non-spherical particulates of the order of 10 μm in size can be observed. Figure 3b shows a higher magnification micrograph of the surface of a particulate. It indicates that the 10 μm sized agglomerates are composed of primary particles of particle size 30-70nm.

Figure 3c is a volume percent against particle diameter histogram of PZT powder that was produced with route A. The diagram show that almost 90 % in volume of the powder consisted of particles with diameter above 5 μm and only 10 % in volume of the powder consists from sub-micron particles.

Figures 4a - 4b are SEM micrographs of examples of PZT powder that was produced using route B and subsequently heat treated at 500 ^{o}C for 1h. In Figure 4a, particle agglomerates of up to 3μm in size with an approximately equiaxed shape can be observed. Figure 4b shows a higher magnification micrograph of free standing agglomerates with diameter 50 - 200 nm and primary particle size 30 - 50nm.

Figure 4c is a particle diameter histogram of PZT powder that was produced using route B and subsequently heat treated at 500 ^{o}C for 1h. The diagram shows that only sub-micron particle formations were detectable in the suspension. The average diameter of particles formations in water is around 250 nm.

Figures 5a - 5b are SEM micrographs of examples of PZT powder that was produced using route B and heat treated at 550 ^{o}C for 24h. Figure 5a shows agglomerates up to 2μm in diameter with approximately equiaxed

shape. The higher magnification micrograph, Figure 5b, shows agglomerated primary particles with a primary particle size similar to the 500 ^{o}C heat treated powder.

Figure 5c is a particle diameter histogram of PZT powder that was produced using route B and heat treated at 550 ^{o}C for 24h. The diagram shows that around 95 % of the total volume of the powder consist from sub-micron formations with mean diameter around 350 nm. About 5 % of the powder volume consists from particles with size 2-3 μm.

Figures 6a – 6c are XRD diagrams of PZT powders that were produced with routes A and B. In Figure 6a a XRD diagram of PZT powder produced with route A and heat treated at 500 ^{o}C for 1h is presented. Comparison with the peaks for pyrochlore and perovskite shows that this route powder is a mixture of pyrochlore and perovskite phases. Figure 6b is a XRD diagram of PZT powder produced with route B and heat treated at 500 ^{o}C for 1h. This is mainly pyrochlore with very little perovskite phase present. In Figure 6c, a XRD diagram of PZT powder produced with route B and heat treated at 550 ^{o}C for 24h is presented. The XRD peaks show that this heat treatment gave a powder with perovskite phase only.

Figures 7a shows heat flow against time curves for the PZT sol and the 1 300 000 MW PVP respectively. The PZT-sol exhibits a shallow endothermic peak between 50–140 ^{o}C followed by two broad exothermic peaks, one at 310–350 ^{o}C and the second at 420–450 ^{o}C. The 1 300 000 MW PVP, exhibits two endothermic peaks one at 50-100 ^{o}C and the second at 420-440 ^{o}C. Figure 7b shows heat flow diagrams for Gel (i) and Gel (ii). Gel (i) exhibits two exothermic peaks one at 320–370 ^{o}C and the second at 410–450 ^{o}C. Gel (ii)

also exhibits two endothermic peaks, one at 40-150 ^{o}C, and the second at 410–450 ^{o}C, as well as two exothermic peaks, the first at 320–370 ^{o}C and the second at 420-450 ^{o}C.

Discussion

From the SEM micrographs it can be observed that all three powders have the same size range of primary particles diameter 30-50 nm. It can be concluded that the extra polymer that was added in the secondary process stage did not significantly affect the size of the primary particles. However, a comparison of figures 3a, 3c and 4a, 4c indicates that the second addition of polymer significantly reduces the agglomerate size.

Comparing the results, it can be hypothesised that by adding extra polymer, as a secondary stage, the PZT particles in the gel were immobilized. As a consequence of this immobilization, the particles were hindered from reacting and creating agglomerated formations of larger particles during the drying and burn out steps. C=O groups of PVP are known to be strongly bonded with OH groups of the metalloxane polymers via hydrogen bonding [31][32]. Such C=O groups can be regarded as the “capping agent” for the OH groups of the metalloxane polymers, obstructing the condensation reaction.

A comparison between XRD figures 6a and 6b shows that similar conditions in the burn out stage resulted in powders with different crystalline phases. The PZT powder that was produced with route A gave a mixture of pyrochlore and perovskite phases. The powder that was produced with route

B did not produce a detectable perovskite phase. These results indicate that an extra amount of PVP can delay the formation of the perovskite phase.

A similar comparison between XRD figures 6b and 6c shows that for the route B powder an increase in the burn out temperature and time produced a completely perovskite phase in the PZT. A comparison of the primary particles morphology in Figures 4b and 5b indicates that the production of the perovskite phase was not at the expense of significant initial sintering of the powder. Figures 4c and 5c show that the increase in the burn out temperature also effects the particle population. The average diameter of the sub-micron particles was increased. Particle formations with diameter above 1 μm were created. This behaviour can be explained by taking in consideration the local sintering that is noticeable in figure 5b. Figure 5b shows that the particles with smother surfaces have also created bridges with their neighbour particles. These hard agglomerates would be correlated with the new population of micron-scale particles.

The role of the PVP in the sol-gel process was investigated using DSC. The common endothermic peak, in Figures 7a and 7b, at 30–150 ^{o}C corresponds to the evaporation of the solvent and the water. The exothermic peak, at 310–370 ^{o}C, is common to all the PZT containing samples and is likely to correspond to the decomposition of the organic species. The exothermic peak exhibited by the PZT sol [Figure 7a] between 420-450 ^{o}C is likely to be caused by the formation of a metastable pyrochlore phase accompanied by the remaining combustion of the organics [33]-[35].

The endothermic peak at 420-450 ^{o}C exhibited by the PVP in Figure 7a corresponds to the melting point of the polymer. Gel (i) also has an

exothermic peak in the temperature range 420–450 ^{o}C but the total released energy was much greater than for the PZT sol sample. This indicates the presence of a different mechanism. The breaking of the hydrogen bonds between the C=O groups of PVP and the OH groups of the metalloxane polymers is likely to provided the extra energy. Gel (ii) exhibits the same behaviour as Gel (i), except for an endothermic peak at 410–450 ^{o}C. The extra amount of polymer, added in the secondary stage, for Gel (ii) is likely to account for this.

The DSC results indicate that the first stage polymer created bonds with the alkoxides and controlled the speed of the condensation reaction. However, the SEM pictures show that the first stage polymer was not able to prevent agglomeration during the drying process. The second stage polymer was necessary to complete the encapsulation of the first stage PZT particles and prevent them from further reaction during the drying and burn out stage.

Conclusions

Two sol-gel routes were used to create PZT powder. Both gave similar primary particles sizes and morphologies but different agglomerate formations. The extra amount of polymer that was added as a secondary stage prevented the formation of large agglomerates and created a powder with sub-micron primary particles. The amount of polymer in the PZT-PVP gel appears to be able to affect the final crystal phase of powder without affecting significantly the size of the freestanding particles.

Acknowledgements

This work would not have been possible without the financial support from EPSRC [grant No: GR/R43303]. The authors would like to thank Professor Roger Whatmore for his helpful discussion of the research results.

References

1. M. N. Rahaman, *Ceramic processing and sintering*, New York, 1995
2. Xue Junmin, John Wang and Toh Weiseng, Synthesis of lead zirconate titanate from an amorphous precursor by mechanical activation, *J. of All. And Comp.*, **308**, p. 139-146, 2000
3. L. B. Kong, W. Zhu, O. K. Tan, Preparation and characterization of $Pb(Zr_{0.52}Ti_{0.48})O_3$ ceramics from high-energy ball milling powders, *Mater. Let.*, **42**, p.232-239, 2000
4. L. B. Kong, J. Ma, R.F. Zhang, W. Zhu, O. K. Tan, Lead zirconate titanate ceramics achieved by reaction sintering of PbO and high-energy ball milled $(ZrTi)O_2$ nanosized powders, *Mater. Let.*, **55**, p. 370-377, 2002
5. Z. Brankovic, G. Brankovic, C. Jovalekic, Y. Maniette, M. Cilense, Mechanochemical synthesis of PZT powders, *Mater. Sci. and Engin.A*, **345**, p. 243-248, 2003

6. R. N. Das, P. Pramanik, Chemical synthesis of nanocrystalline lead zirconate-titanate powders using tartarate precursor, *Mater. Lett.*, **40**, p. 251-254, 1999

7. R. N. Das, R. K. Pati, P. Pramanik, A novel chemical route for the preparation of nanocrystalline PZT powder, *Mater. Lett.,* **45**, p. 350-355, 2000

8. Li Guo, A. Lyashchenko, Xian-Lin Dong, Synthesis of zirconium-rich PZT ceramics by hydroxide coprecipitation under hot-press, *Mater. Lett.,* **56**, p. 849-855, 2002

9. Gang Xu, W. Weng, J. Yao, P. Du, G. Han, Low temperature synthesis of lead zirconate titanate powder by hydroxide co-precipitation, *Microelec. Engin.,* **66**, p. 568-573, 2003

10. B. Guiffard, M. Troccaz, Low temperature synthesis of stoichiometric and homogeneous lead zirconate titanate powder by oxalate and hydroxide coprecipitation, *Mat. Resear. Bull.,* **33**, p. 1759-1768, 1998

11. I. R. Abothu, Shi-Fang Liu, S. Komarneni, Q. H. Li, Processing of $Pb(Zr_{0.52}Ti_{0.48})O_3$ (PZT) ceramics from microwave and conventional hydrothermal powders, *Mat. Resear. Bull.,* **34**, p. 1411-1419, 1999

12. M. Traianidis, C. Courtois, A. Leriche. Mechanism of PZT crystallisation under hydrothermal conditionsDevelopment of a new synthesis route, *J. of the Europ. Ceram, Societ.*, **20**, p. 2713-2720, 2000

13. M. Traianidis, C. Courtois, A. Leriche, B. Thierry, Hydrothermal synthesis of lead zirconium titanate (PZT) powders and their characteristics, *J. of The Europ. Ceram. Societ.,* **19**, p. 1023-1026, 1999

14. Seung-Beom Cho, M. Oledzka, R. E. Riman, Hydrothermal synthesis of acicular lead zirconate titanate (PZT), *J. of Cryst. Growth.*, **226**, p. 313-326, 2001

15. B. Fegley, E. A. Barringer, Synthesis and characterisation of monosized doped TiO_2 powders, J. Am. Ceram. Soc., **67**, p. 113-116, 1984

16. Xiaoheng Liu, An improvement on sol-gel method for preparing ultrafine and crystallized titania powder, *Mat. Sci. and Engin.A*, **289**, p.241-245, 2000

17. An-Wu Xu, The Preparation, Characterization, and their Photocatalytic Activities of Rare-Earth-Doped TiO_2 Nanoparticles, *J. Of Catalysis*, **207**, p. 151-157, 2002

18. Yang Chuanfang, Production of ultrafine ZrO_2 and Y-doped ZrO_2 powders by solvent extraction from solutions of perchloric and nitric acid with tri-n-butyl phosphate in kerosene, *Powder Technology*, **89**, p. 149-155, 1996

19. Sei-ichi Suba, Synthesis of $MgO–SiO_2$ and $CaO–SiO_2$ amorphous powder by sol–gel process and ion exchange, *J. Non-Cryst. Sol.*, **255**, p. 178-184, 1999

20. Takashi Ogihara, Hirohisa Kaneko, Nobuyasu Mizutani, Preparation of monodispersed lead zirconate-titanate fine particles, *J. of Mater. Scin. Let.*, **7** , p. 867-869, 1988

21. Q. F. Zhou, Nanocrystalline powder and fibres of lead zirconate titanate prepared by the sol-gel process, *J. of Mater. Proc. Tech.*, **63**, p. 281-285, 1997

22. C.D.E. Lakeman, D. A. Payne, Processing effects in the sol-gel preparation of PZT dried gels, powders, and ferroelectric thin-layers, *J. Am. Ceram. Soc*, **75**, p. 3091-3096, 1992

23. W. D. Yang., PZT/PLZT ceramics prepared by hydrolysis and condensation of acetate precursors, *Ceram. Intern.,* **27**, p.373-384, 2001

24. L. Weng, X. Bao, K. Sagoe-Crentsil, Effect of acetylacetone on the preparation of PZT materials in sol–gel processing, *Mat. Sci. And Engin.B*, **96**, p. 307-312, 2002

25. Fu-Ping Wang, Yan-Ju Yu, Zhao-Hua Jiang, Lian-Cheng Zhao, Synthesis of $Pb_{1-x}Eu_x(Zr_{0.52}Ti_{0.48})O_3$ nanopowders by a modified sol–gel process using zirconium oxynitrate source, *Mater. Chem. And Phys.,* **77**, p. 10-13, 2002

26. H. Brunckova, L. Medvecky, J. Briancin, K. Saksi, Influence of hydrolysis conditions of the acetate sol–gel process on the stoichiometry of PZT powders, *Ceramics. International.*, **30***,* p 453-460, 2004

27. Hiromitsu Kozuka, Atsushi Higuchi, Single-layer submicron-thick $BaTiO_3$ coatings from PVP-containing sols: Gel-to-ceramic film conversion, densification, and dielectric properties, *J. Mater. Res.*, **16**, p. 3116-3123, 2001

28. Young Ho Rho, Kiyoshi Kanamura, Minori Fujisaki, Jun-ichi Hamagami, Sei-ichi Suda, Takao Umegaki, Preparation of $Li_4Ti_5O_{12}$ and $LiCoO_2$ thin film electrodes from precursors obtained by sol–gel method, *Solid State Ionics,* **151**, p.151-157, 2002

29. Mao-ping Zheng, Ming-yuan Gu, Yan-ping Jin, Hong-hua Wang, Pin-fang Zu, Ping Tao, Ji-bao He, Effects of PVP on structure of TiO_2 prepared by the sol-gel process, *Mat. Sci. and Engin B*. **87**, p. 197-201, 2001

30. Franck Rataboul, Ce´line Nayral, Marie-Jose´ Casanove, Andre´ Maisonnat, Bruno Chaudret, Synthesis and characterization of monodisperse zinc and zinc oxide nanoparticles from the organometallic precursor $[Zn(C_6H_{11})_2]$, *J. Organ. Chem*., **643–644**, p. 307-312, 2002

31. H. Kozuka, M. Kajimura, Single – Step Dip Coating of Crack– ree $BaTiO_3$ Films > 1 μm Thick: Effect of Poly(vinylpyrrolidone) on Critical Thickness, *J. Am. Ceram. Soc.,* **83**, p. 1056-62, 2000

32. Hiromitsu Kozuka, Atsushi Higuchi, Single–layer submicron–thick $BaTiO_3$ coatings from poly(vinylpyrrolidone)–containing sols: Gel–to–ceramic film conversion, densification, and dielectric properties, *J. Mater. Res.,* **16**, p. 3116-3123, 2001

33. Aiying Wu, Isabel M. Miranda Salvado, Paula M. Vilarinho, João L. Baptista, Lead Zirconate Titanate Prepared From Different Zirconium and Titanium Precursors by sol-gel, *J. Am. Ceram. Soc,* **81,** p. 2640-2644, 1998

34. Y.Z. Chen, J. MA, L. B. Kong, R.F. Zhang, Seeding in sol-gel process for $Pb(Zr_{0.52}Ti_{0.48})O_3$ powder fabrication, *Mat. Chem. and Phys.,* **75**, p. 225-228, 2002

35. Aiying Wu, Paula M. Vilarinho, Isabel M. Miranda Salvado, João L. Baptista, Sol – Gel Preparation of Lead Zirconate Titanate Powders and

Ceramics: Effect of Alkoxide Stabilizers and Lead Precursors, *J. Am. Ceram. Soc.,* **83**, p. 1379-1385, 2000

Figures captions.

Figure 1. Preparation route of PZT-PVP gel.

Figure 2a. Preparation route A for PZT powder. No PVP was added as a secondary stage.

Figure 2b. Preparation route B for PZT powder. PVP was added as a secondary stage.

Figure 3a. SEM micrograph of PZT powder. No PVP was added as secondary stage. Burn out at 500 ^{o}C for 1h.

Figure 3b. SEM micrograph of PZT powder. No PVP was added as secondary stage. Burn out at 500 ^{o}C for 1h.

Figure 3c. Size distribution in volume of PZT powder. No PVP was added as secondary stage. Burn out at 500 ^{o}C for 1h.

Figure 4a. SEM micrograph of PZT powder. PVP added as secondary stage. Burn out at 500 ^{o}C for 1h.

Figure 4b. SEM micrograph of PZT powder. PVP added as secondary stage. Burn out at 500 ^{o}C for 1h.

Figure 4c. Size distribution in volume of PZT powder. PVP added as secondary stage. Burn out at 500 ^{o}C for 1h.

Figure 5a. SEM micrograph of PZT powder. PVP added as secondary stage. Burn out at 550 ^{o}C for 24h.

Figure 5b. SEM micrograph of PZT powder. PVP added as secondary stage. Burn out at 550 ^{o}C for 24h.

Figure 5c. Size distribution in volume of PZT powder. PVP added as secondary stage. Burn out at 550 ^{o}C for 24h.

Figure 6a. XRD diagram of PZT powder. No PVP was added as secondary stage. Burn out at 500 ^{o}C for 1h.

Figure 6b. XRD diagram of PZT powder. PVP added as secondary stage. Burn out at 500 ^{o}C for 1h.

Figure 6c. XRD diagram of PZT powder. PVP added as secondary stage. Burn out at 550 ^{o}C for 24h.

Figure 7a. DSC diagrams of PZT sol and PVP polymer with average molecular weight 1 300 000

Figure 7b. DSC diagrams of PZT-PVP gel (i) and PZT-PVP gel (II).

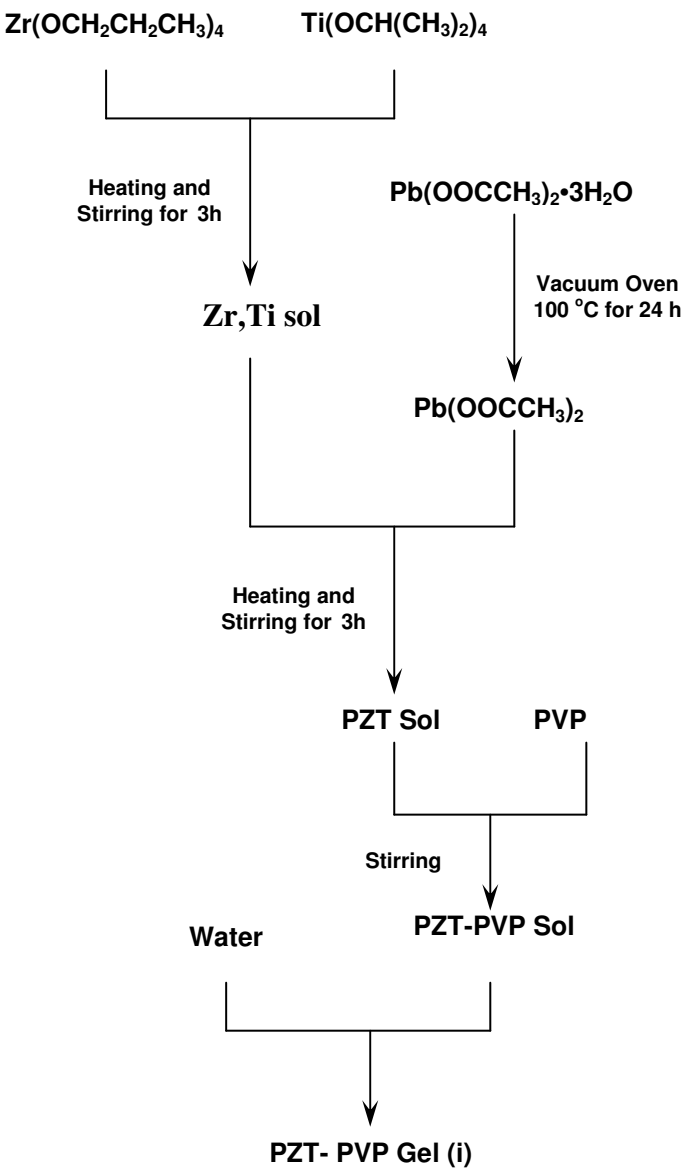
Zr(OCH2CH2CH3)4
Ti(OCH(CH3)2)4
Heating and Stirring for 3h
Pb(OOCCH3)2•3H2O
Vacuum Oven 100 °C for 24 h
Zr,Ti sol
Pb(OOCCH3)2
Heating and Stirring for 3h
PZT Sol
PVP
Stirring
Water
PZT-PVP Sol
PZT- PVP Gel (i)

Figure 1.

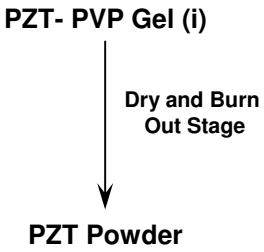

Figure 2a.

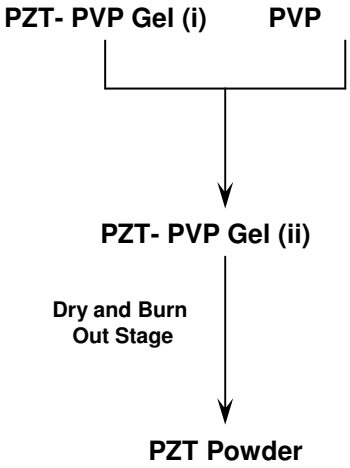

Figure 2b.

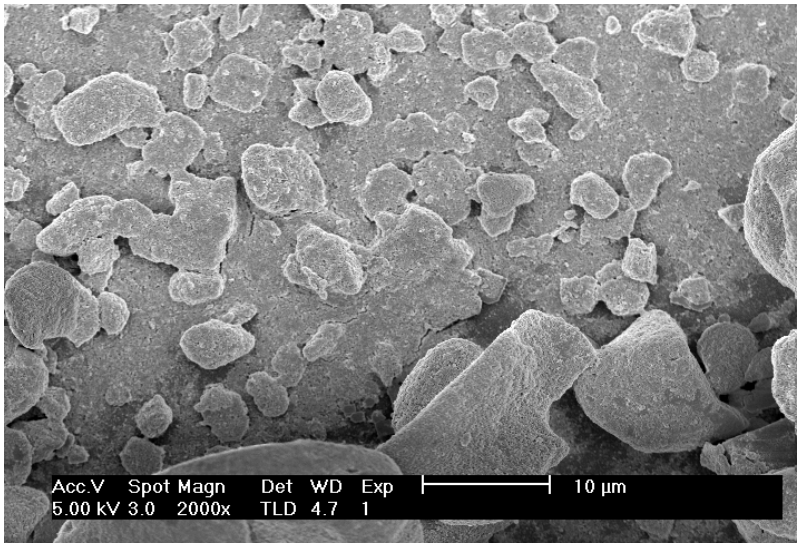

Figure 3a.

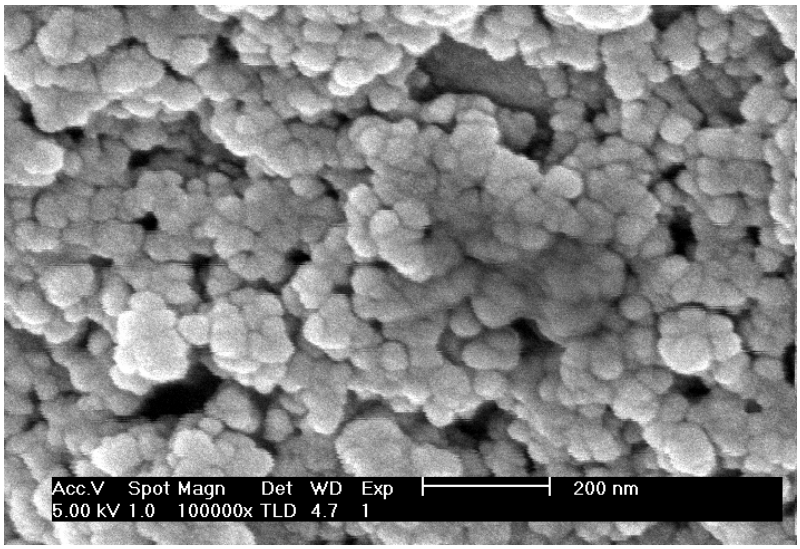

Figure 3b.

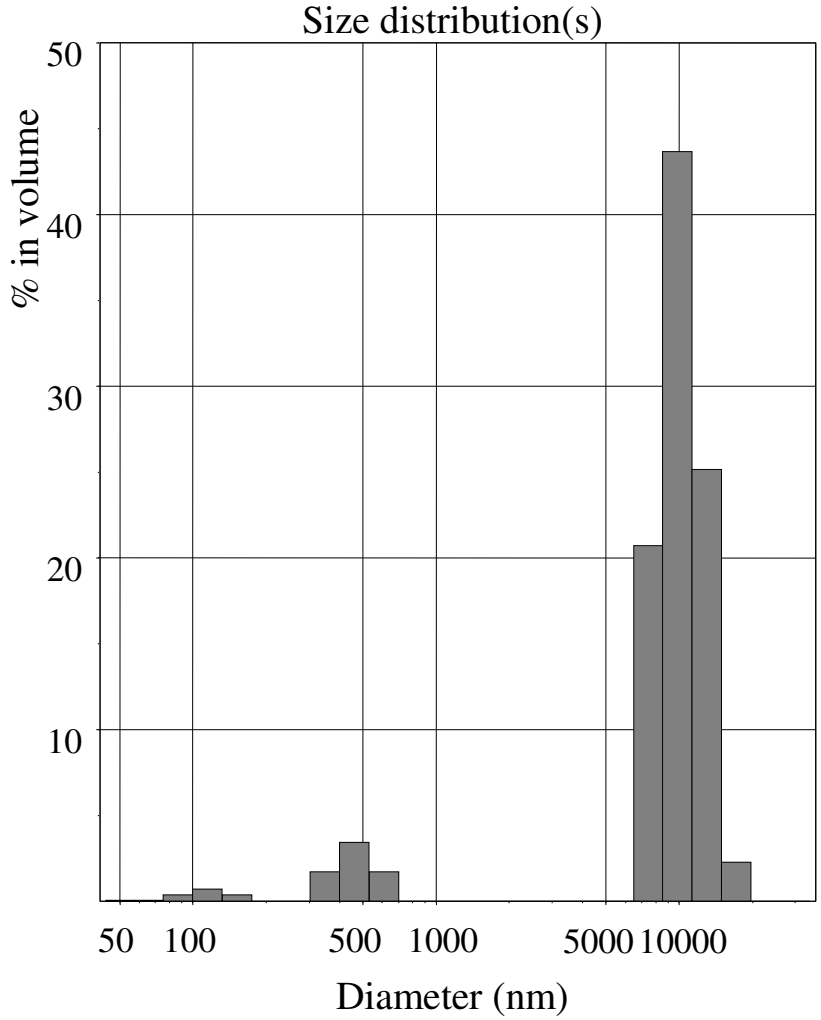
Size distribution(s)
% in volume
50
40
30
20
10
50
100
500
1000
5000
10000
Diameter (nm)

Figure 3c

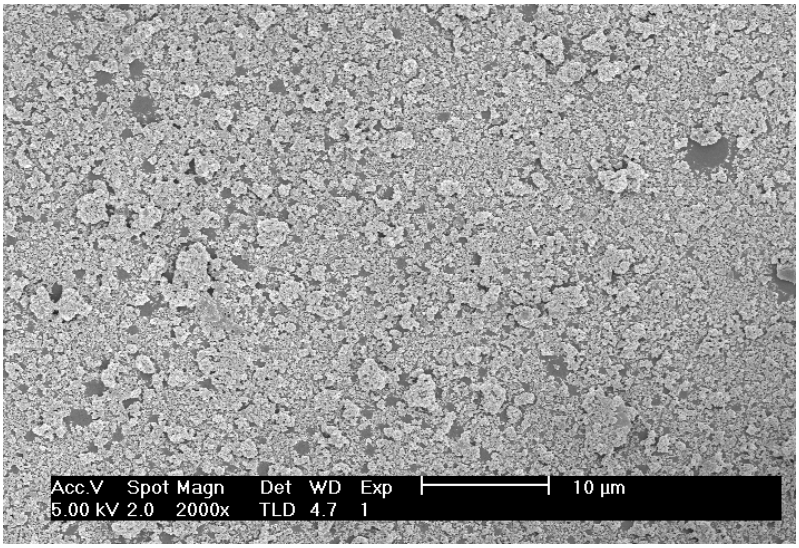

Figure 4a.

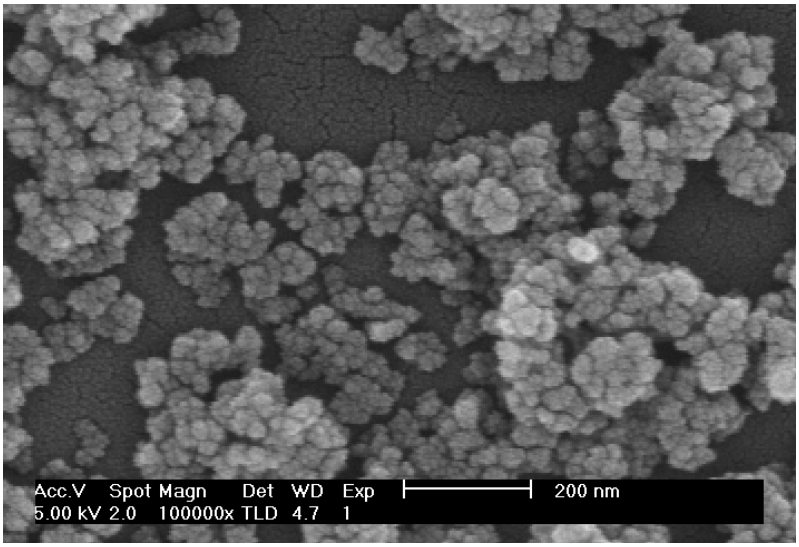

Figure 4b

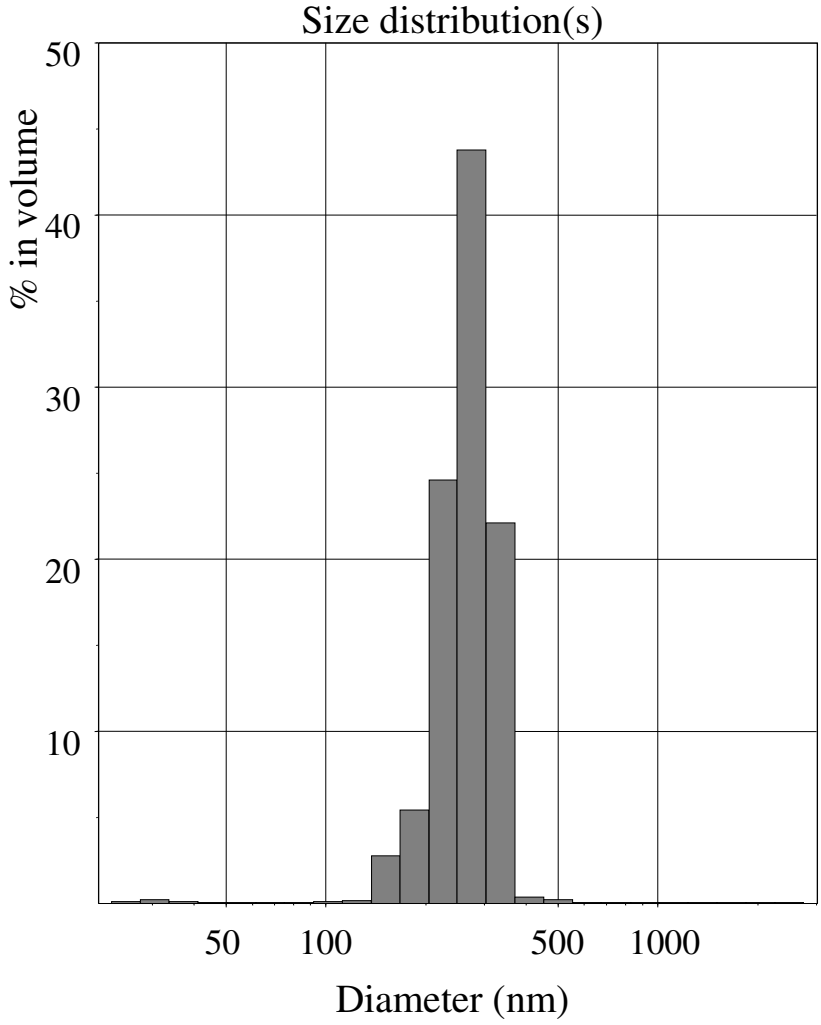
Size distribution(s)
% in volume
50
40
30
20
10
50
100
500
1000
Diameter (nm)

Figure 4c

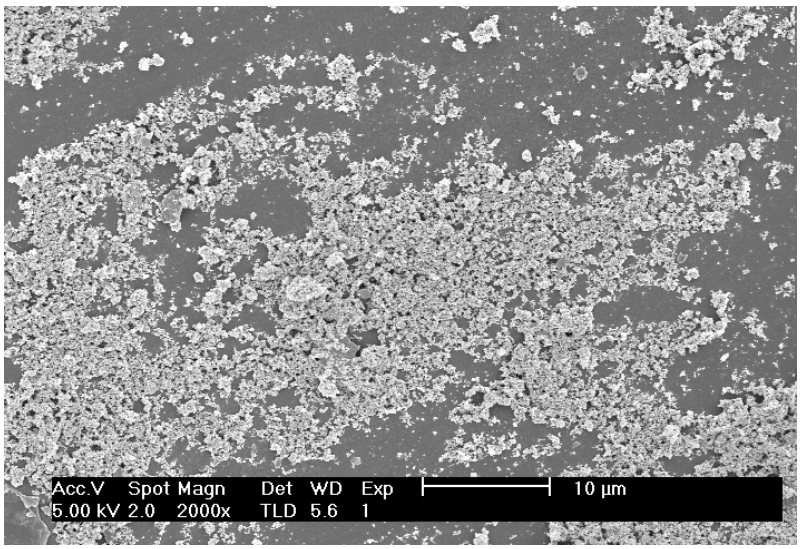

Figure 5a.

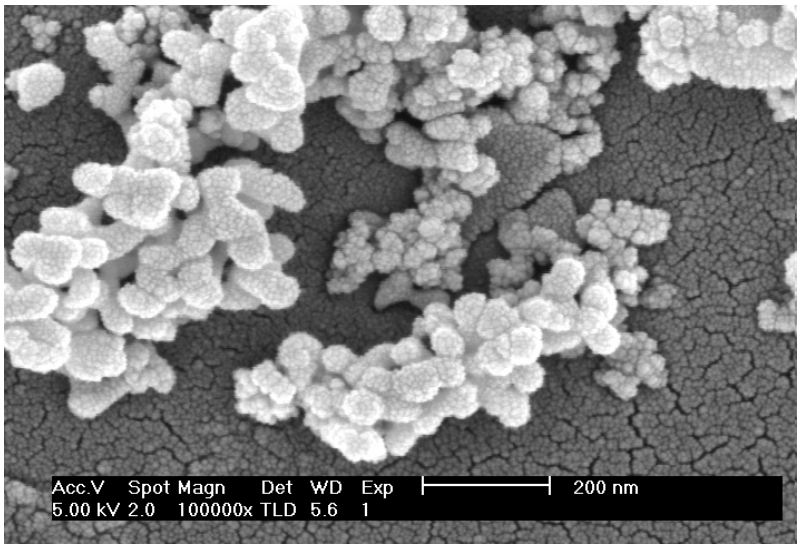

Figure 5b

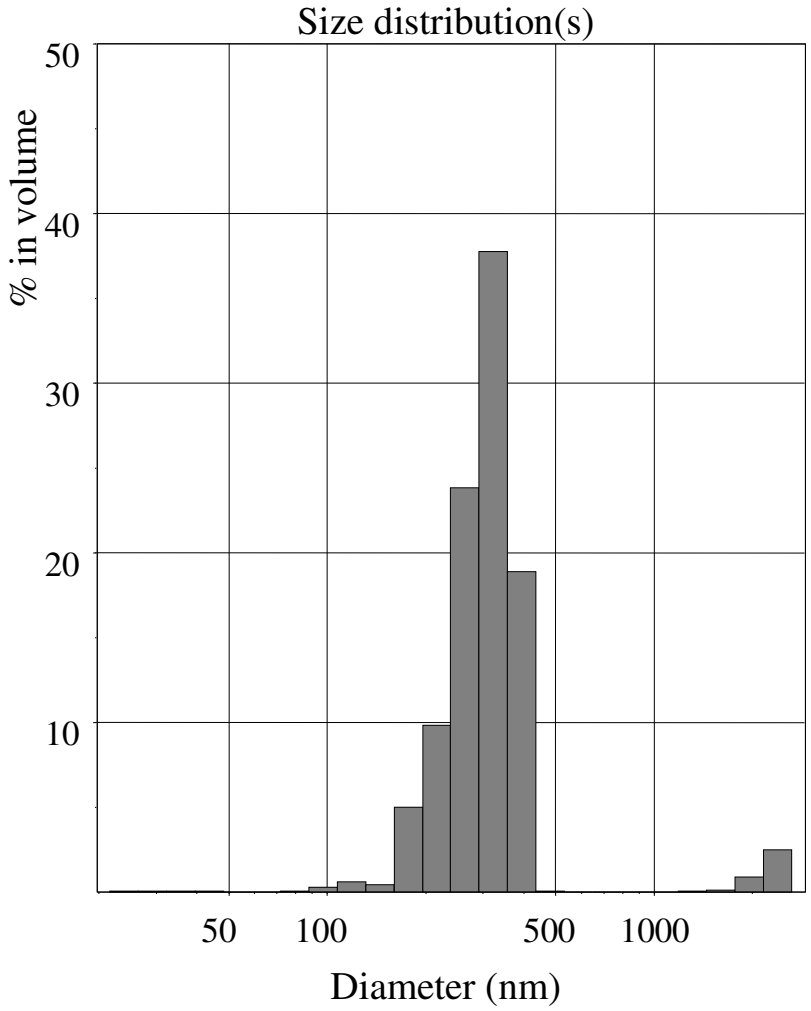
Size distribution(s)
% in volume
50
40
30
20
10
50
100
500
1000
Diameter (nm)

Figure 5c

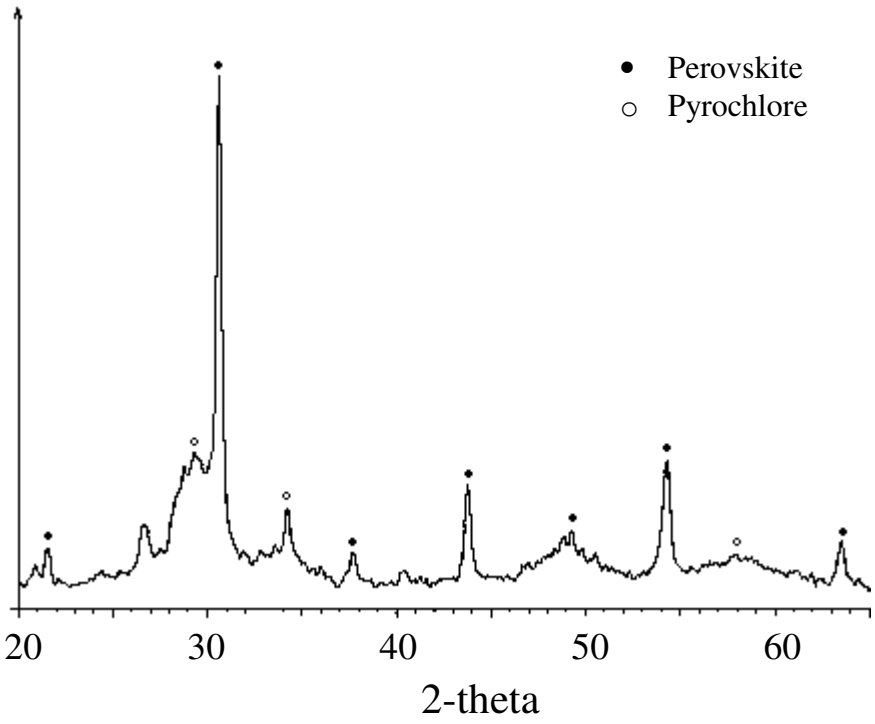

Figure 6a

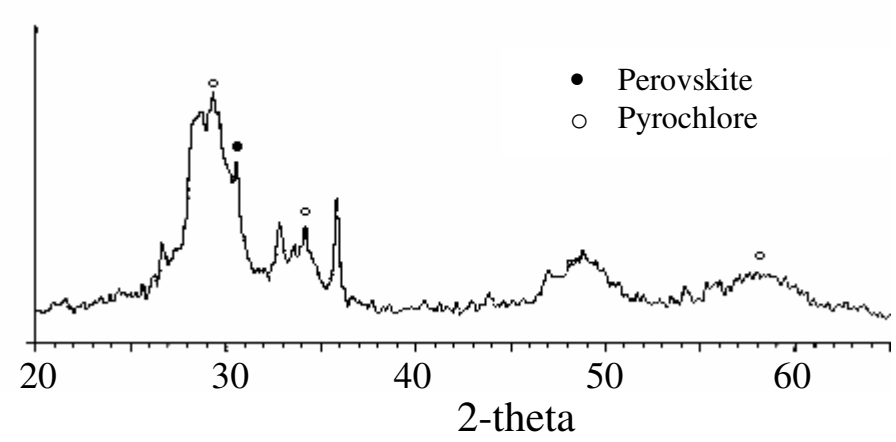

Figure 6b

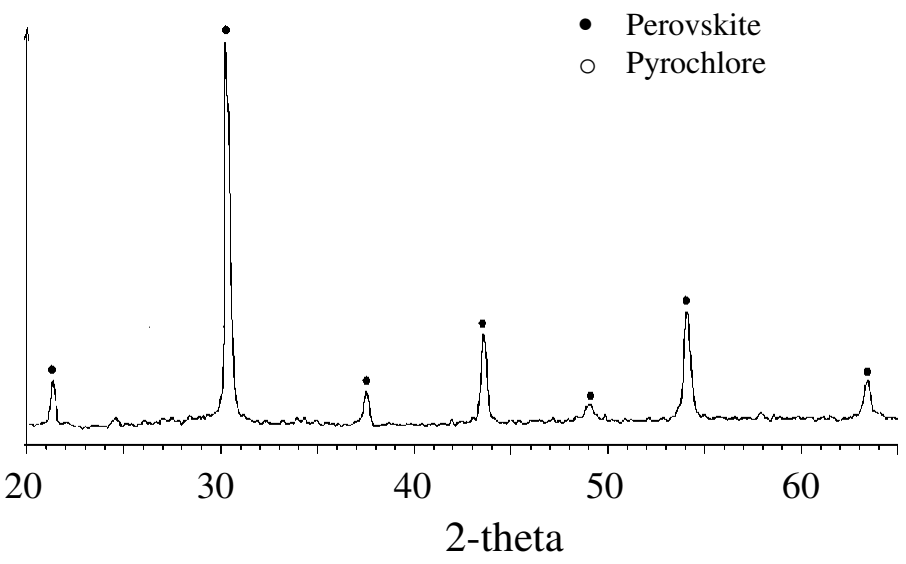

Figure 6c

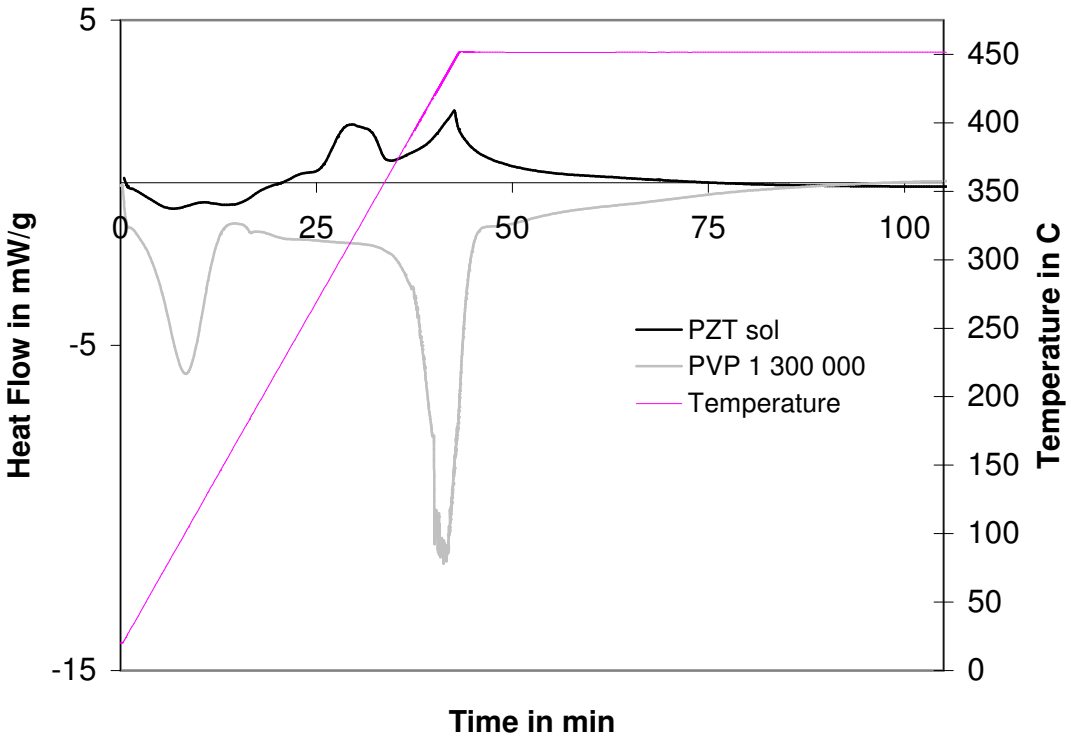

Figure 7a

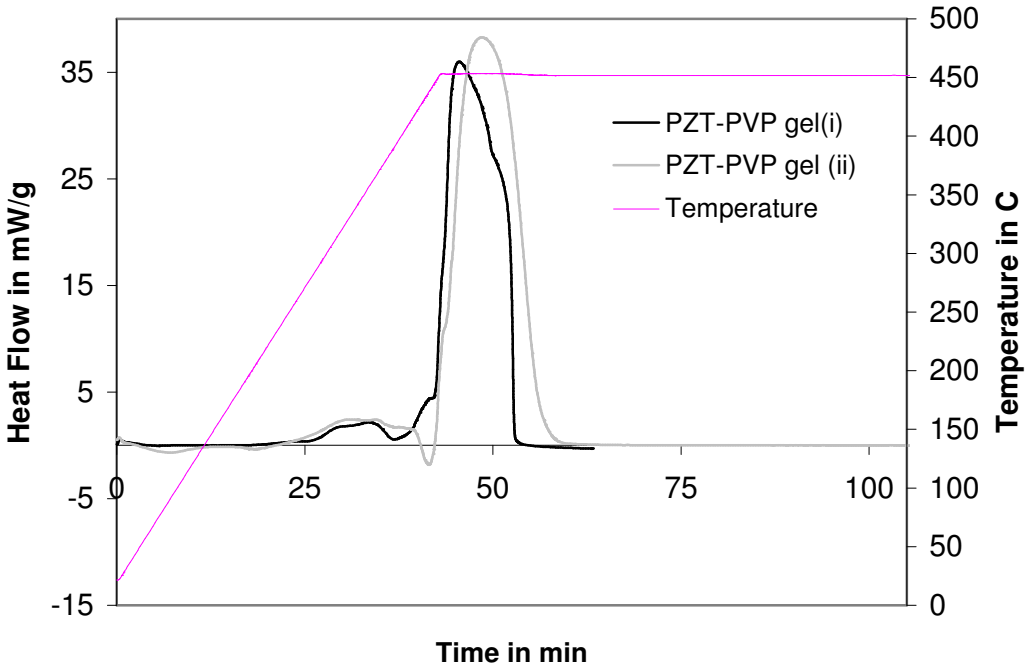
Heat Flow in mW/g
35
25
15
5
-5
-15
0
25
50
75
100
500
450
400
350
300
250
200
150
100
50
0
Temperature in C
Time in min
PZT-PVP gel(i)
PZT-PVP gel (ii)
Temperature

Figure 7b